# SIGNIFICANCE OF MORPHODYNAMIC REGIME IN MEANDERING RIVER

**Dr. N.L. Dongre, IPS, Ph.D., D.Litt****

**Meandering Indus River which is a smaller river till then became a bigger river due to the inclusion of water from Sutlej.**

***Abstract:*** *This is an attempt to correlate theoretical and experimental results on the issue of two-dimensional morphodynamic influence with field data from natural single-thread rivers. Theoretical and experimental study has expressed that two-dimensional planform and bed deformation waves can explain both upstream and downstream within single-thread meandering rivers. The existence of upstream influence is controlled by the value of channel aspect ratio with respect to a threshold that is determined by reach-averaged characteristics and by the evolutionary state of a given river section. It is explored that the predictions of a mechanistic meander simulation model based on the input of field data referring to more than 100 gravel bed rivers in order to quantify the regime of morphodynamic influence that can be expected in these streams. The analysis points out how the predicted morphodynamic regime of a given reach can be controlled by the bankfull aspect ratio and the Shields stress. Differences within the data set suggest an autogenic tendency of gravel bed rivers to behave superresonantly, while environmental factors like denser vegetation and reduced gravel supply tend to promote the subresonant regime. Moreover, the autogenic tendency of developing meanders to continuously modify their sinuosity and to consequently reduce the down-channel slope almost invariably promotes transition from the superresonant to the subresonant regime.*

---

**Dr. N.L. Dongre
C-14 Jaypee Nagar Rewa 486450
Email: - nl.dongre@jalindia.co.in dongrenl@gmail.com
Mobile No. 7869918077, 09425152076

**Keyword:** Single-thread rivers, morphodynamic regime, Meandering Rivers.

## INTRODUCATION

[2] Significant developments in the morphodynamics of meandering, single-thread rivers have been influenced through enhanced learnings from geomorphological research of meander dynamics *[Hooke,* 1995; *Gay et a!.,* 1998; *Hooke,* 2003; *Frothingham and Rhoads,2003;* Hooke,2007a; *Gautier et al.,* 2007] and modeling depended on kinematics *[Ferguson,* 1984] or fluid mechanics (e.g., *Ikeda et al.* [1981], *Blondeaux and Seminara* [1985], *Crosato* [1989], *Seminara and Tubino* [1992], *Howard* [1996], *Sun et al.* [2001], and the recent review of *Seminara* [2006].

[3] Latest numerical models of meandering processes [e.g., *Chen andDuan,* 2006; *Ruther and Olsen,* 2007] have been validated with experiments carried out under laboratory conditions [e.g., *Struiksma et al.,* 1985; *Colombini et al.,* 1992; *Nagata et al.,* 1997; *Zolezzi et al.,* 2005] depend on field evidence, although a few quantitative and enlightening comparisons have been performed *[Darby et al.,* 2002]. A closer comparison is undoubtedly rather difficult to achieve, but at the same time it would mark a major step forward in our knowledge of fluvial processes.

[4] This article is focused on the issue of 2-D morphodynamic influence, on which only recently a certain degree of convergence has been achieved after decades of shifting interpretations *[Mosselman et al.,* 2006]. This concept has been developed referring to meandering rivers, but actually, it can be extended to the broader class of alluvial, single-thread streams.

[5] In the experiments of *Struiksma et al.* [1985] on erodible channels with constant curvature and fixed banks, the presence of a bend connecting two straight reaches was shown to produce a morphodynamic effect in the downstream direction, which displays itself in the form of a steady, nonmigrating alternate bar pattern which was invariably absent in the upstream straight reach. This is an example of downstream morphodynamic influence. A few years later, *Zolezzi and Seminara* [2001] theoretically predicted the existence of upstream influence, which can take place only in wider and shallower channels, characterized by higher width to depth ratios.

This picture has been experimentally confirmed by *Zolezzi et al.* [2005], who also indicated that downstream influence characterizes both types of streams, regardless of the value of the aspect ratio $\beta$. In more general terms, the phenomenon of 2-D morpho-dynamic influence consists of the longitudinal propagation of a transverse (scour deposition) bed deformation triggered by a geometric disturbance such as a discontinuity in channel curvature. The channel aspect ratio $\beta$ emerges as the controlling parameter for this phenomenon. Upstream influence takes place only when $\beta$ falls above a threshold value ("wide" channels) while downstream influence is experimentally observed in both wide and "narrow" channels. The threshold aspect ratio $\beta_R$is determined in a rather complex way by reach-averaged hydraulic, geometrical and sediment conditions and it coincides with the` resonant value of *Blondeaux and Seminara* [1985]; therefore, it separates two distinct regimes of morphodynamic influence, which are called superresonant and subresonant, respectively.

[6] The previous examples are actually exemplifications of a much broader category of morphodynamic effects associated with the direction of propagation of morphodynamic influence in single thread, natural channels with irregular plan-form geometry *[Seminara et al.,* 2001; *Lanzoni and Seminara,* 2006]. This picture has relevant implications for river management and restoration purposes *[Kondolf,* 2006], since morphodynamic influence is triggered by geometrical disturbances related to both anthropogenic and natural factors, and it affects the flow bed topography field and consequently the planimetric evolution of the river. This is due to the presence and propagation of both planform and two-dimensional bed deformation waves, which propagate information associated with changes in boundary conditions along the channel *[Lanzoni et al.,* 2006]. This picture is also relevant for planimetric evolution models of river meanders since it allows to establish the correct positioning and number of boundary conditions that need to be imposed at the ends of the longitudinal domain *[Lanzoni and Seminara,* 2006].

[7] The purpose of the present study is to understand whether single thread natural channels may be dominantly characterized by one of these two influence regimes. Although not providing field evidence of the occurrence of the morphodynamic regimes, a first attempt is made to answer the following key questions. Do gravel bed stream reaches fall entirely in the subresonant regime, entirely in the superresonant regime, or do both situations occur? Which allogenic and autogenic factors control the morphodynamic regime of a river? And finally, is the morpho-dynamic regime of a gravel

bed meandering river dependent on its evolutionary state and therefore possibly subject to changes at certain timescales? The latter question relates to the gradual changes of reach-averaged conditions determined by progressive elongation of meander bends, which eventually leads to a reduction in channel slope, which in turn changes the reach-averaged parameters and therefore the $\beta_R$ value. This may imply that the morpho-dynamic regime can change because of planimetric evolution, an effect which has never been investigated in detail.

[8] The analysis has focused on gravel bed, single-thread rivers, for which a relatively wide and tested data set from different geographical locations is available *[Parker et al.,* 2007]. It is used that these field data as input conditions for the morpho-dynamic model of *Zolezzi and Seminara* [2001] which has recently been recognized as belonging to a class of models incorporating the most relevant physical effects among linear meander simulators *[Camporeale et al.,* 2007; *Lanzoni et al.,* 2006].

[9] In section 2 it is summarized the most relevant features of meander resonance and of the two morpho-dynamic regimes. In section 3 it is described the planimetric evolution model and illustrate the field data set. Results are discussed in sections 4 and 5, and a final summary together with the open issues for future work concludes the paper.

## 2. Regimes of Morphodynamic Influence in Meandering Rivers

[10] We briefly review the main properties of the two morphodynamic regimes starting from an overview of the resonance phenomenon which theoretically characterizes the linear solution of the flow bed topography field in the morphodynamics of single-thread channels and defines the threshold separating between them.

[11] The resonant behavior arises when investigating the linear stability of a straight channel with constant representative water discharge *(Q*),* width *(W*),* slope *(S)* and median sediment size *($d_{50}$*)* with respect to a regular, sine-generated perturbation of the channel axis. Note that a star (*) hereinafter will denote dimensional quantities. The investigation of meander dynamics through the bend stability process was originally proposed by *Ikeda et al.* [1981] and has subsequently been improved by relating meander growth rate to a progressively more complete description of in-stream morphodynamics, accounting for the full coupling between bed deformation and flow field. Assuming sediment transport to be in equilibrium with the representative hydraulic parameters leads to the selection of one preferential meander wavelength which corresponds to the maximum growth rate of the perturbations. The amplitude of the oscillations tends to infinity or, in other words, resonates, for well defined values $(\lambda_R, \beta_R)$of the wave number and of the channel width to depth ratio *[Blondeaux and Seminara,* 1985]. Such behavior is purely theoretical and related to the linear solution of the 2-D morphodynamic model which presents the typical structure of linear oscillators, and can therefore be subject to resonance of the solution.

[12] Although meander dynamics is characterized by both flow *[Seminara and Tubino,* 1992] and geometrical *[Hooke,* 2003; *Perucca et al.,* 2005] nonlinearities, the linear approximation has allowed great insight in the mechanics of meander dynamics in the past decades [e.g., *Ikeda et al.,* 1981; *Struiksma et al.,* 1985; *Johannesson and Parker,* 1989; *Seminara and Tubino,* 1989; *Crosato,* 1990]. A sample outcome is given in Figure 1, which describes the stability and migration properties of an indefinitely long sequence of regular, sine-generated meander bends with small amplitude in dependence of meander wave number $\lambda$ and channel width ratio $\beta$, defined as

$$\lambda = \frac{\pi W^*}{L^*};\ \beta = \frac{W^*}{2D^*} \tag{1}$$

with *W*, D** average channel width and depth, and *L** one full meander wavelength.

[13] The picture arising from Figure 1 can be qualitatively reproduced by a variety of second- or higher-order linear models, including among others *Struiksma et al.* [1985], *Johannesson and Parker* [1989], and *Seminara and Tubino*[1989].

[14] Unstable meanders are defined as those growing in time thus leading to mature meander forms, while the perturbed amplitude of stable bend sequences tends to be damped and the corresponding sine-generated planform to

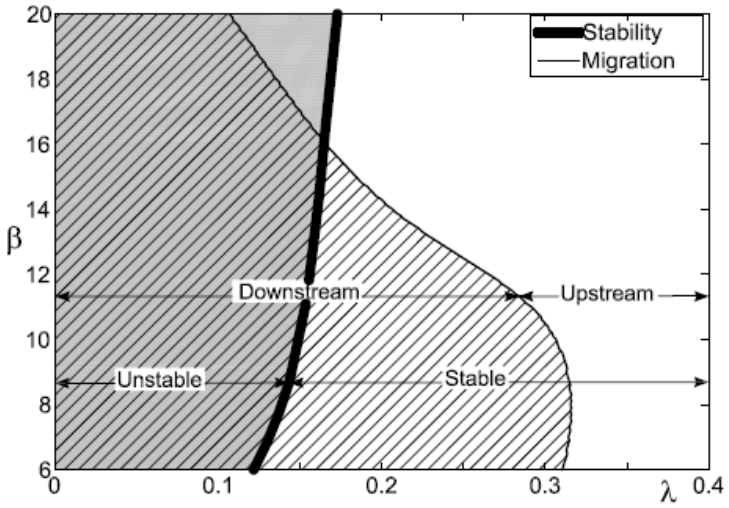


**Figure 1. Marginal stability and migration curves of small-amplitude meandering rivers in the ($\lambda - \beta$) plane ($\tau* = 0.1$, $d_s = 0.05$). Meander growth and downstream migration occur in the grey shaded area with stripes, while upstream migration of growing meander bends occur in the shaded region (approximately of triangular shape) without stripes. All meanders whose wave number exceeds the value corresponding to the thick continuous line are linearly stable and tend to rectify. Resonant conditions ($\lambda_R$, $\beta_R$) are defined by the intersection of the marginal curves.**

be straightened. The wave number of the perturbation appears as the most important parameter discriminating between stable and unstable forms: only long enough meander wavelengths, say longer than 15 times channel width, are likely to evolve toward mature meander loops, nearly regardless of the value of the width ratio $\beta$.In contrast, $\beta$ appears to be a major control on the possibility that unstable meanders migrate upstream: this can happen only if $\beta > \beta_R$, with subresonant meander bends($\beta < \beta_R$) invariably propagating planform waves in the downstream direction.

[15] Besides corresponding to the linearly maximum amplification, it appears that resonant conditions more importantly represent a threshold separating two morpho-dynamic regimes. That threshold also occurs in analyses that incorporate geometric *[Lanzoni and Seminara,* 2006] and flow nonlinearities *[Nobile et al.,* 2008] and it has been confirmed by experimental observations *[Zolezzi et al.,* 2005]. Meanders characterized by different regimes have different planimetric and altimetric dynamics. Superresonant meanders migrate upstream and are skewed downstream in their mature evolution stage; the opposite applies for sub-resonant meanders. Moreover, the morphodynamic influence of sharp geometric disturbances is only felt downstream in subresonant meanders, and also upstream only in superresonant channels *[Zolezzi et al.,* 2005].

[16] According to the theory and to other linear models of the same class (like those of *Struiksma et al.* [1985] and *Johannesson and Parker* [1989]) upstream influence can therefore only occur in superresonant streams; however, it must be noted that in real rivers other effects, not accounted for in these models, can cause upstream influence and upstream meander migration also under subresonant conditions. First, both 1-D and 2-D flow patterns are affected by backwater effects. Second, alternate bars and point bars may grow in upstream direction due to the stalling of coarse sediments in situations close to the initiation of motion. Thirdly, meanders in relatively steep valleys with significant subsurface flows may migrate upstream because bank destabilization due to groundwater seepage occurs mainly upstream of the bend apices.

[17] A physical explanation for the variation in 2-D morphodynamic influence in the subresonant and super-resonant regimes can be provided through an analogy with the well established one-dimensional case *[De Vries,* 1965; *Lyn and Altinakar,* 2002]. Here critical conditions correspond to unit Froude number; upstream influence, occurring also in supercritical flows, is due to the possibility that small amplitude one dimensional bed and/or free surface waves travel in the upstream direction. In the two-dimensional context, small amplitude morphodynamic waves take the form of linear migrating river bars whose direction of migration is controlled by marginal curves that result from classical linear stability analyses [e.g., *Kuroki and Kishi,* 1985; *Colombini et al.,* 1987; *Garcia and Nino,* 1993]. Bar migration, as well as bar growth, is controlled by a delicate balance between

opposing effects related to the phase lag of the bed load flux with respect to bed deformation. Linear bar stability analyses reveal that unstable, small amplitude bars (therefore growing in time) can migrate in the upstream direction only in the superresonant regime($\beta < \beta_R$)which therefore defines the range of channel aspect ratios in which 2-D morphodynamic influence can be expected. The non-linear growth of migrating bars eventually suppresses their upstream migration, whose numerical as well as laboratory observation is not straightforward and requires a careful experimental design. These observations on the possible upstream movement of small amplitude migrating bars can be used to explain physically why in the two-dimensional framework the width ratio $\beta$ replaces the Froude number as the parameter discriminating whether upstream influence can occur. Variations of $\beta$ across the resonant threshold are able to substantially modify the phase lag between the spatial divergence of the bed load flux and the pattern of bed topography *[Zolezzi and Seminara,* 2001].

[18] Furthermore, *Lanzoni and Seminara* [2006], recognizing that meanders develop as a result of an instability process, have mathematically demonstrated that such instability is mostly of convective nature [e.g., *Briggs,* 1964]. This means that a small, unstable perturbation of the channel axis localized in space develops into a group of meander waves which grow and migrate: the wave group is eventually convected away from its initial location leaving the original planform unperturbed. The group velocity of meander perturbation changes sign as the resonant barrier is crossed: meander migration shifts from downstream to upstream as $\beta$ increases and becomes larger that $\beta_R$.

[19] Note that since resonance is related to the homogeneous solution of the governing differential problem, the related concepts of morphodynamic influence are not strictly related to the meandering planform of the channel but apply in general to single-thread, alluvial channels.

[20] Field observations *[Hooke,* 2007a] indicate the relevance of these findings to understanding the mechanisms and propagation of morphodynamic changes in meandering rivers, and also raise the crucial question of to what extent meander dynamics can be determined by autogenic or allogenic factors *[Hooke,* 2007b].

[21] Direct evidence of the above behaviors in natural meandering streams has not been achieved so far. The opportunities to directly compare field data with mathematical models are often restricted by the time scale of available field observations; this is generally limited to a maximum of several tens of years with few exceptions when old cartographic maps are available *[Hooke and Redmond,* 1989]. Moreover, simulation models often rely on necessary simplifying assumptions which may tend to underestimate the variety of geomorphic and anthropic controls which determine what is actually observed in the field.

[22] Herein it is tried to link theoretical models with field observations by assessing what leads an alluvial, single-thread gravel bed river to self select its own mor-phodynamic influence regime and by eventually identifying primary controls that may determine the choice of one or of the other.

## 3. Methods and Data

### 3.1. Mathematical Model: Resonance and Planimetric Evolution

[23] The mathematical model employed in the present work is basically made of two main ingredients: a flow bed topography model for single-thread meandering channels with given distribution of channel curvature, and a planimetric evolution equation *[Seminara et al.,* 2001], whose time integration assumes that the flow and bed topography instantaneously adapt to planform changes occurring on longer timescales.

[24] The flow bed topography model is needed to compute the morphodynamic regime of a stream given its reach-averaged characteristics (section 4). The planimetric evolution model allows investigation of the extent to which a meandering stream can modify its own morphodynamic regime in dependence of its planimetric evolution stage (section 5).

[25] The model inputs are reach-averaged conditions, which can be represented by the three dimensionless parameters $\beta$ (equation (1)),, $\tau *, d_s$ where

$$d_s \frac{d_{50}^*}{D_0^*}; \tau_* = \frac{S}{\Delta d_s}, \tag{2}$$

with $d_s$ the relative roughness and $\tau^*$ the bankfull Shields stress for which the uniform flow expression has been used. In (2) $D_0^*$ denotes the reach-averaged uniform flow depth, $d_{50}^*$ the median grain diameter, and $S$ the longitudinal slope of the fluvial reach, $\Delta$ the relative submerged sediment density, for which the standard value 1.65 has been assumed.

[26] The flow bed topography model basically consists of the linear solution of the depth averaged 2-D momentum and continuity equations for water and sediments, along with appropriate closure relationships for flow resistance and bed load intensity. The model assumes constant channel width, uniform sediment size, transport of sediments occurring mainly as bed load, which are typical assumptions of linear meander models.

[27] The model actually belongs to a class of linear models that have been described in a variety of contributions [e.g., *Bl ndeaux and Seminara,* 1985; *J hanness n and Parker,* 1989; *Cr sat* , 1990; *Z lezzi and Seminara,* 2001] which are based on the laws of mass and momentum conservation governing fluid mechanics within open channel flows with movable boundaries (bed and banks) and therefore fully account for meander mechanics (flow properties, bed deformation, channel migration although in a rather simplified way). Gaining insight into the relevant physical mechanisms is actually a major strength of this kind of models, since each physical effect has a correspondent term in the equations, which can be quantified as soon as the equation is solved. Existing mechanistic models may differ for the adopted assumptions, which may result in varied model performance: the work of *Camp reale et al.* [2007] is a good review of how different linear meander models account for the several physical effects controlling meander mechanics. The description of channel morphodynamics based on these type of models has been received experimental validation in several applications [e.g., *Struiksma et al.,* 1985; *Z lezzi et al.,* 2005].

[28] Models of this kind also differ for the mathematical technique used to solve the differential and algebraic equations that result from the conservation laws. The solution technique in the present case is based on perturbation expansions, which allow obtaining approximate, asymptotic behaviors of the solution when some relevant parameters are small (typically the ratio between channel width and the radius of curvature in the case of meanders). Although approximate, the power of solutions based on perturbation analysis is their requirement of very small computation efforts while at the same time replicating observed behaviors, which easily allows quantifying the relative weight of the physical effects that are accounted for in the model. From this it is possible to build the link between the physics and observed/replicated behaviors.

[29] We now briefly recall the features of the planimetric evolution equation of main relevance for the present analysis.

[30] if $\vartheta$ denotes the local inflexion angle, formed between the local tangent to the channel centerline with the down-valley direction, then the planimetric evolution of the channel is described by the following in tegrodifferential equation *[Seminara et al.,* 2001]:

$$\vartheta_{,T} - \vartheta_{,s} \int_0^s \zeta \vartheta_s ds = \zeta_{,s.} \tag{3}$$

In (3), $T$ is time and $\zeta$(s) represents the lateral migration rate at a given cross section *s.* The longitudinal distribution $\zeta$(s) is assumed to adapt almost instantaneously to changes in meander planform; the present model assumes a rather simplified, albeit classical [e.g., *Ikeda et al.,* 1981; *Hasegawa,* 1989], bank erosion law which linearly relates the channel migration rate to the excess near-bank longitudinal velocity. It is worth pointing out that this simplification does not account in detail for the processes actually governing bank stability, and also implicitly assumes the river width to be constant in time, an approximation that is nevertheless acceptable for the purposes of the present study.

[31] The ubiquity of regular meandering patterns in natural rivers *[Kinoshita,* 1961; *Langbein and Leopold,* 1964] has often led to a search for periodic solutions of (3), corresponding to a theoretically indefinite sequence of identical and periodic meander loops. Under these conditions channel planform is described through the classical "Kinoshita curve," which reveals the dominance of odd harmonics (typically the first and the third) in the distribution of channel curvature. Herein we have incorporated also possible multilobing effects triggered by the fifth harmonic, and expanded the inflexion angle $\vartheta(s,T)$as well as the migration rate $\zeta(s;T)$as follows *[Seminara et al.,* 2001]:

$$(\zeta,\vartheta)=\sum_{k=1,3,5}\vartheta_k\,(T)\big(\zeta_{k'}1\big)\exp[i\,\curlywedge_k\,(T)s]+\mathrm{CC},$$

$$\curlywedge_k=\frac{\pi k}{L^*(T)/W^*}=k\,\curlywedge\,(T), \tag{4}$$

where CC is the complex conjugate. The expression (4) reflects the presence of only odd harmonics in the distribution of channel curvature, which is implicit in the cubic nonlinearity of (3), and also assumes that $|\vartheta_k| \gg |\vartheta_{k+2}|$ In (4) $\curlywedge_k$ is the dimensionless wave number of each (odd) harmonic of the chosen expansion. It is rather well established that the geometry of individual meander bends can be described through a sine generated curve whereby channel curvature distribution is represented by the sum of sine functions including mainly odd harmonics (first, third, and fifth). The significance of the first and third harmonic has been widely discussed in previous work [e.g., *Kinoshita,* 1961; *Parker et al.,* 1983], while the fifth harmonic accounts for the presence of multilobing that characterizes some meander loops at the mature stage of evolution. The link with the actual morphodynamics can be found in the development of riffle pool sequences that generate in relative straight reaches of meandering channels eventually giving rise to additional or "multiple" loops. Describing the actual complexity of sediment transport patterns associated with these processes is beyond the scope of the present work, although it can be provided on the basis of the employed morphodynamic model.

[32] The planimetric evolution equation (3) reduces to the following ordinary differential system for the first, the third and the fifth harmonic of the expansion (4) and for the evolution of meander wave number $\curlywedge$:

$$\frac{d\theta}{dT}=\mathbf{F}(\theta,\zeta,\mathrm{CC});\ \ \mathbf{F}=\big(\mathcal{F}_1,\mathcal{F}_3,\mathcal{F}_5\big), \tag{5}$$

$$\zeta=\big(\zeta_1,\zeta_3,\zeta_5\big),\ \theta=\big(\vartheta_1,\vartheta_3,\vartheta_5\big),$$

$$\frac{d\curlywedge}{dT}=\curlywedge^2\,[i(5\bar{\zeta}_5\,\vartheta_5\bar{\vartheta}_5+3\bar{\zeta}_3\,\vartheta_3\bar{\vartheta}_3+\bar{\zeta}_1\,\vartheta_1\bar{\vartheta}_1)+\mathrm{CC}], \tag{6}$$

where bold characters denote vectors, an overbar denotes the conjugate of a complex number and $\mathcal{F}_1,\mathcal{F}_3,\mathcal{F}_5$ are complex algebraic expressions reported by *Seminara et al.*[2001].

[33] Equation (6) is particularly relevant for the present work, since the function $\curlywedge\,(T)$describes the progressive elongation of the channel that takes place during meander evolution. This causes a gradual reduction of down-channel slope stays constant at the timescale of planimetric evolution. This mechanism is responsible for the variation of reference conditions that control the river morphodynamic regime.

[34] Assuming uniform flow in morphodynamic equilibrium as reference conditions, the governing dimensionless parameters $\beta,\ T^*, d_s$vary from their initial values ($T$ =0) on the slow timescale of planimetric evolution, according to the evolution of channel sinuosity $\sigma(T)$:

$$[\beta(T,),\tau_*(T)]=[\beta(0),\tau_*(0)]\sigma-\frac{3}{10}(T)$$

$$d_s(T)=d_s(0)\sigma-\tfrac{7}{10}(T). \tag{7}$$

As a consequence, the value of the resonant width ratio $\beta_R$also varies during planimetric evolution. In many gravel bed rivers the bed load function $\Phi$ is only dependent on the Shields stress while flow roughness can be assumed to depend mainly on the normalized water depth (neglecting its dependence on $\tau^*$, which would arise in the presence of dunes or of other small-scale bed forms). Under these conditions, the approximate following relationship holds for $\beta_R$ *[Camporeale et al.,* 2007]:

$$B_R=\frac{\pi}{2}\left[\frac{r}{C_{f0}\sqrt{\tau_*0}[C_D+2\Phi_T-3]}\right]^{\frac{1}{2}}. \tag{8}$$

In (8), $C_D$ and $\Phi_T$ express the normalized variations of the friction factor $C_f$ and of the dimensionless intensity of bed load $\Phi$ with the flow depth $D^*$ and with the Shields parameter $\tau_*$, respectively:

$$C_D = \frac{D_0^*(T)}{C_{f0}(T)} \frac{\partial C_f}{\partial D^*}\Big|_0 \; ; \; \Phi_T = \frac{\tau_{*0}(T)}{\Phi_0(T)} \frac{\partial \Phi}{\partial \tau_*}\Big|_0 . \tag{9}$$

Moreover, the subscript zero refers to reach averaged conditions; the quantities $C_{f0}, \tau_0, C_D, \Phi_T, \Phi_0$ are time-dependent, $r \simeq 0.5$ to $0.6$ expresses the gravity effect on the direction of sediment transport, $C_{f0}$ is the reference friction factor.

[35] In the following, we have used a classical logarithmic closure to compute $C_{f0}$, $C_D$:

$$C_f = \left[6 + 2.5\, In \frac{D^*}{2.5\, d_5^*}\right]^{-2}, \tag{10}$$

and we have employed the formula of *Parker* [1990] to calculate the quantities $\Phi_0$, $\Phi_T$. In order to assess the sensitivity of our results to the choice of the empirical bed load predictor we have further tested our results against the choice of other two well known formulae for bed load transport *[Meyer-Peter and Muller,* 1948; *Bagnold,* 1980].

### 3.2. Input Data Set

[36] The computation of the morphodynamic regime requires the knowledge of reach-averaged representative values of flow discharge, channel width, water depth, down-channel slope and mean sediment size. It is assumed that bankfull channel geometry as representative conditions for the medium-to long-term morphodynamics and have referred to a data set containing the reach-averaged bankfull properties of a series of single-thread rivers. The data set for bankfull geometry of alluvial gravel bed streams includes a total of 134 rivers. It is composed of the following five subsets: (1) 16 river reaches in Alberta, Canada reported by *Kellerhals et al.* [1972] and, in more detail, by *Parker* [1979]; (2) 23 river reaches in Idaho *[Parker et al.,* 2003]; (3) 10 river reaches of the Colorado River, western Colorado and eastern Utah *[Pitlick and Cress,* 2000]; (4) 23 river reaches in Britain *[Charlton et al.,* 1978]; and (5) 62 river reaches in India compiled by *N.L. Dongre.*

[37] In the following, we will refer to two main subsets: North American (NA) subset includes Alberta, Idaho, and Colorado subsets, while United Kingdom (UK) subset includes the other ones. These data subsets have been recently used by *Parker et al.* [2007] to determine a series of dimensionless relations for the bankfull hydraulic geometry of alluvial gravel Bed Rivers. The relations that have been derived show a considerable degree of universality. They can be cast in the following vectorial form:

Table 1. Range of Variation of the Dimensional and Dimensionless Parameters Relative to River Reaches Belonging to the UK and NA Subdata Sets

| | Number | $Q^*$(m3/s) | $W^*$ (m) | $D_0^*$ (m) | $d_{50}^*$ (mm) | S(%) |
|---|---|---|---|---|---|---|
| UK rivers | 85 | 27-550 | 5.2-77.1 | 0.50-4.19 | 14-176 | 0.07-2.1 |
| NA rivers | 49 | 3.4-5440 | 5.6-280 | 0.25-6.95 | 27-167 | 0.03.3.1 |
| | $\beta$ | | $\tau_*$ | | $d_s$ | |
| 90th percentile | 12.5 | | 0.084 | | 0.100 | |
| UK mean | 8.5 | | 0.050 | | 0.051 | |
| 10th percentile | 4.8 | | 0.024 | | 0.021 | |
| 90th percentile | 25.9 | | 0.082 | | 0.194 | |
| NA mean | 15.6 | | 0.044 | | 0.088 | |
| 10th percentile | 8.4 | | 0.015 | | 0.011 | |

$$\left(\overline{W},\, \breve{D}, S\right) = \left(a_w, a_D, a_s\right) \hat{Q}^{(n_W n_D, n_S)}, \tag{11}$$

Where

$$\left(\breve{W},\ \breve{D}\right) = \frac{g^{1/5}}{Q^{*2/5}}\left(W^*, D^*\right);\ \hat{Q} = \frac{Q^*}{\sqrt{g d_s^{*3}}}. \quad (12)$$

In (11), g is gravity acceleration, $a_W$ =4.63, $a_D$ = 0.382, $a_S$ = 0.101 and $n_W$ = 0.0667 ± 0.027, $n_D$ = -0.0004 ± 0.027, $n_S$ = 0.344 ± 0.066 *[Parker et al.,* 2007].

[38] Minimum and maximum values of the bankfull discharge *Q*,* width *W*,* depth *D*,* of the mean grain size $d_{50}^*$ and of the channel slope S are reported in Table 1 for the UK and the NA subsets. Despite substantial differences within the two subsets *[Hey and Thorne,* 1986], dimension-less reach averaged values of $\beta$, $\tau_*$ and $d_s$ (equation (2)) indicate significant differences between the two subsets. NA reaches have a much larger mean aspect ratio ($\beta$ = 15.6) than UK reaches ($\beta$ = 8.5), meaning they are much wider and relatively shallower. This feature had already been noticed [e.g., *Parker et al.,* 2007] and related to a denser riparian vegetation favored by a more humid climate in the UK, as well as to a reduced sediment supply with respect to rivers in the NA data set. A second relevant feature is the relative low average value of the shields stress $\tau*$ for both the NA and UK subdata sets (0.044 to 0.050), which nearlycoincides with the threshold for sediment motion adopted by the classical formula of *Meyer-Peter and Miiller* [1948]. As already noted by *Parker et al.* [2007], the average value of the Shields stress at incipient sediment motion is lower, tending to oscillate around the value 0.03; this consideration must indeed apply if accepting that most alluvial gravel bed rivers are competent to move their median surface size at bankfull flow. It is therefore used the bed load predictor of *Parker* [1990] whereby Φ and $\Phi_T$ are continuous functions of $\tau*$,making it particularly suitable for mathematical treatment within prediction models.

[39] Note that when examining possible changes in the morphodynamic regime due to meander planimetric evolution (section 5) it is restricted that the analysis only to those rivers whose sinuosity value is reported in the data sets. This has resulted in a strong preference for reaches within the UK subdata set. For computation performed in section 5 a total of 86 river reaches have been taken into account as follows: (1) 10 river reaches in Alberta, Canada reported by *Parker* [1979]; (2) 19 river reaches in the UK reported by *Charlton et al.* [1978]; and (3) 57 river reaches compiled by *Hey and Thorne* [1986].

## 4. Prevalent Superresonant Regime of Single-Thread, Gravel Bed Rivers

[40] The complete solution of the flow bed topography model and the approximate relationship (8) are used to predict the resonant conditions for the 134 gravel bed river reaches belonging to the chosen data set. Quantitative differences between the exact and the approximate computations are lower than 5% and all the results presented below are almost independent of this choice. Subresonant (super-resonant) reaches correspond to $\beta < \beta_R$( $\beta > \beta_R$), while we have referred to near-resonant river reaches when the absolute value of the difference ($\beta$ —$\beta_R$) is lower than 10% $\beta_R$.

[41] In Figure 2a NA Rivers are denoted by triangles while UK streams are represented by circles. The distinction between subresonant and superresonant reaches clearly appears from the legend. Theoretical $\beta_R$ ($\tau*$) curves corresponding to the 10th and 90th percentiles of $d_s$values within the data set are also reported.

[42] Most gravel bed river reaches (96, corresponding to 71% of the sample) are predicted to be superresonant, while 25 (19%) are subresonant; only 13 river reaches (10%) are Moreover, little overlap exists between the two regimes for given values of the bankfull Shields stress: this implies a well defined and relatively narrow transitional aspect ratio range separating subresonant from superresonant regimes which is only slightly dependent on $\tau*$.

[43] Figure 3 shows the values of $\beta$ and of $\beta_R$for the examined river reaches in the form of box plots. The picture arising from Figure 3a is particularly interesting: a very sharp threshold (dashed grey line) appears to separate river reaches falling in the two regimes. Ninety percent of the subresonant reaches display values of the width ratio that do not exceed 7.2; in addition only 10 percent of the super-resonant rivers have an aspect ratio lower than 7.3.

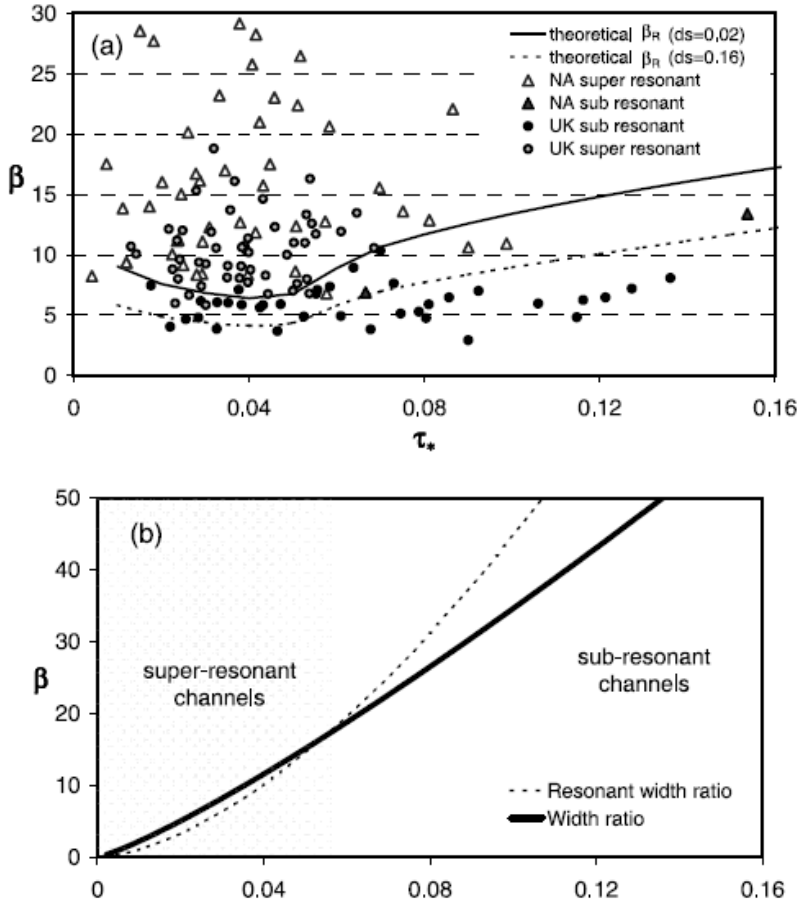


**Figure 2. (a) Bankfull morphodynamic regimes of the examined gravel bed river reaches in the $\beta - \tau*$ parameter space. NA rivers are denoted by triangles while UK streams are represented by circles. (b) The $\beta(\tau*)$ and $\beta_R(\tau*)$ curves resulting from the quasi-universal bankfull geometry relationship proposed by *Parker et al.* [2007].**

Overall, computed resonant values from the whole data set cover a much wider interval, with values of $\beta_R$ for subresonant rivers falling between 5 and 14 (Figure 3b). The existence of such a narrow range of the width ratio separating subresonant and superresonant regime is not obvious at all, and it might provide a simple aspect-ratio-based criterion for a preliminary field assessment of the morphodynamic regime of a river reach. A second relevant control parameter on the morphodynamic regime is the Shields stress $\tau*$Figure 2a indicates that 14 out of 20 (70%) reaches with $\tau*$> 0.07 are subresonant.

[44] It is tested that how general could be the correspondence of the subresonant regime with higher bankfull Shields stress, as suggested by the application of the model to the chosen data sets. For this purpose it is used that the quasi-universal equations proposed by *Parker et al.* [2007] to derive $\beta(\tau*)$ and $\beta_R$ $(\tau*)$ relationships. It is pointed out that many relationships have been proposed to characterize hydraulic geometry on the basis of rational approaches that assume some kind of extremal hypothesis [e.g., *Millar,* 2005; *Eaton et al.,* 2004], and of empirical approaches [e.g., *Van den Berg,* 1995]. *Parker et al.* 's [2007] equations are particularly suitable for the purposes of the present work since they allow $\beta$ and $\beta_R$ to be expressed as functions of only $\tau*$. From (11) and (12) it is possible to derive a relation that links the bankfull width ratio with the Shields stress in the following form:

$$\beta = a\beta^{\tau_*^{n\beta}};\ a_\beta = \frac{a_W}{2a_D a_\vartheta^{n\beta}}\ n_\beta = \frac{n_W - n_D}{n_\vartheta}. \qquad (13)$$

[45] Using the same approach, by manipulating (8) through (11) and (12) and including a suitable frictional

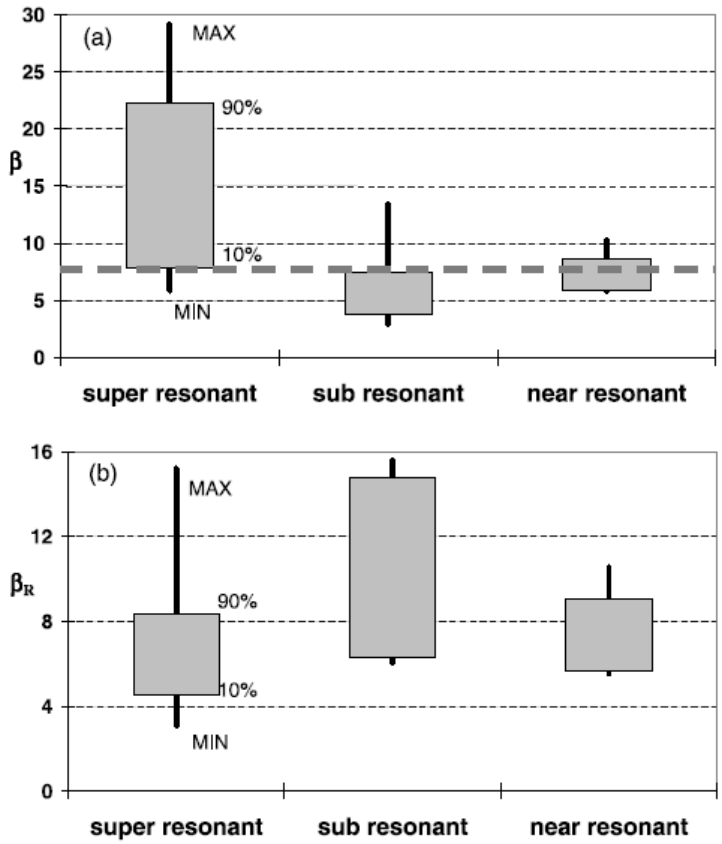


**Figure 3**. **Box plots (a) for $\beta$ and (b) for $\beta_R$. For each category the grey boxes indicate the values of the 10th and of the 90th percentiles; the upper and the lower vertical lines extend to the maximum and minimum values of the category.**

resistance law (like equation (20a) of *Parker et al.* [2007]), it is possible to derive an analogous "quasi-universal" $\beta_R(\tau*)$ relation for gravel bed rivers, that reads

$$\beta_R = a_R \tau_*^{nR},$$
$$a_R = \frac{\pi}{2}\left[\frac{r a_r^2}{(-2n_r + 2\Phi_T - 3) a_D^{-2n_r} a_\vartheta^{\frac{2n_r}{n_\vartheta}\left(nD+\frac{2}{5}\right)}}\right]^{1/2}, \quad (14)$$
$$n_R = \frac{n_r}{n_\vartheta}\left(n_D + \frac{2}{5}\right) - 0.25,$$

with $a_r$= 3.671, $a_\vartheta$ = 0.0233, $n_r$ = 0.263 and $n_\vartheta$= 0.0561 [from *Parker et al.,* 2007, equations (34a), (34d), and (38)]. The two relationships are plotted in Figure 2b and show the quasi-universal tendency of gravel bed rivers to super-resonance at low Shields stresses, which reverses for higher $\tau*$, still within the limit of sediment transport occurring dominantly as bed load. The threshold value of $\tau*$ for which the transition is expected may vary according to the predictor employed to calculate $\Phi_T$, but the final outcome is not qualitatively affected.

[46] Table 2 shows how the estimate of morphodynamic regimes varies between the UK and NA subsets. This estimate is not qualitatively affected by the choice of different bed load predictors. Indeed, although quantitatively modifying the reported percentage values, changing the bed load formula preserves the strong prevalence of superresonant reaches within the NA subset, while UK rivers are more well balanced between the two regimes. The differences observed in the UK and NA data subsets allow hypotheses to be formulated on which factors can be responsible for the morphodynamic regime of a gravel bed river, bearing in mind that several differences also exist within each subset, although these are not accounted for in the present study. As already noted by

*Charlton et al.* [1978] and by *Hey and Thorne* [1986], rivers in the UK subdata sets are subject to a more humid climate which facilitates the presence of denser bank vegetation. This is expected to increase bank strength *[Millar,* 2000] and can therefore be responsible for a more pronounced confinement of channel width. A second element, also pointed out by *Parker et al.* [2007], is the likelihood that NA streams have a larger gravel supply than UK river reaches with comparable water discharge.

[47] On the basis of these considerations it is apparent that denser bank vegetation and reduced gravel supply can be factors that promote the subresonant regime in gravel bed rivers, which in the majority of cases would instead tend to fall in the superresonant regime in a state of unaltered sediment supply and with relatively low-vegetation and

**Table 2. Prediction of Morphodynamic Regimes in the UK and NA Subdata Sets Based on Three Different Bed Load Predictors**

| | Superresonant | | | Subresonant | | |
|---|---|---|---|---|---|---|
| | Parker [1990] | Bagnold [1980] | Meyer-Peter and Miiller [1948] | Parker [1990] | Bagnold [1980] | Meyer-Peter and Miiller [1948] |
| UK | 63% | 46% | 44% | 37% | 54% | 56% |
| NA | 94% | 89% | 71% | 6% | 11% | 29% |

low-cohesion side banks. These factors not only can cause the channel to be narrower and deeper, but also have an important role in increasing the threshold $\beta_R$, which tends to remain relatively low in gravel bed rivers, due to the typically large values of the relative roughness $d_s$ and the low values of the Shields stress $\tau*$ (Table 1). This tendency, however, is contrasted in the narrower reaches (like, in the average, in the UK subset), where subresonance is also due to lower values of $d_s$, responsible for higher values of $\beta_R$. Moreover, it is checked that the average size of channels, quantified through the bankfull discharge, does not play a relevant role in the observed difference between the two subsets.

[48] Finally, we have tested how the computation of resonance conditions is affected by the choice of different bed load predictors. All the results presented above have been obtained using the bed load predictor of *Parker* [1990]. Figure 4 compares the relative distance from resonant conditions $(\beta - \beta_R)/\beta_R$obtained using the *Meyer-Peter and Miiller* [1948], the *Bagnold* [1980] and the *Parker* [1990] predictors. It can be seen that changing the bed load formula does not produce any difference in the prediction of the morphodynamic regime, with the exception of two river reaches for the *Bagnold* [1980] formula and of two reaches for the *Meyer-Peter and Miiller* [1948] formula. The estimate of the $\beta_R$ value can be slightly different depending on the bed load formula that is used, especially for subresonant streams (Figure 4). The apparent discrepancy with the outcomes presented in Table 2 is explained by pointing out that percentage values in Table 2 are calculated referring to different totals, since the use of threshold-based formu-laes like those of *Bagnold* [1980] and of *Meyer-Peter and Miiller* [1948] restricts the comparison to those streams with bankfull $\tau*$ that is large enough to exceed the critical values indicated by *Meyer-Peter and Miiller* [1948] and *Bagnold* [1980] for sediment motion. The number of UK reaches available for the computation of resonant conditions passes from82to37*[Bagnold,* 1980] and to 36 *[Meyer-Peter and Miiller,* 1948], while the corresponding number of NA reaches shifts from 52 to 18 *[Bagnold,* 1980] and to 17 *[Meyer-Peter and Miiller,* 1948].

[49] All the above considerations indicate that the key outcomes of the present work are not dependent on the closure used to evaluate bed load transport, and this supports the generality of the results presented above.

## 5. Morphodynamic Regime in Evolving Meandering Rivers

[50] Results presented in the previous paragraph provide a "static" picture of the morphodynamic regime of the river reaches within the UK andNA subsets. Alluvial single-thread channels, however, may tend to evolve their planform and to develop mature meander forms, with a progressive increase

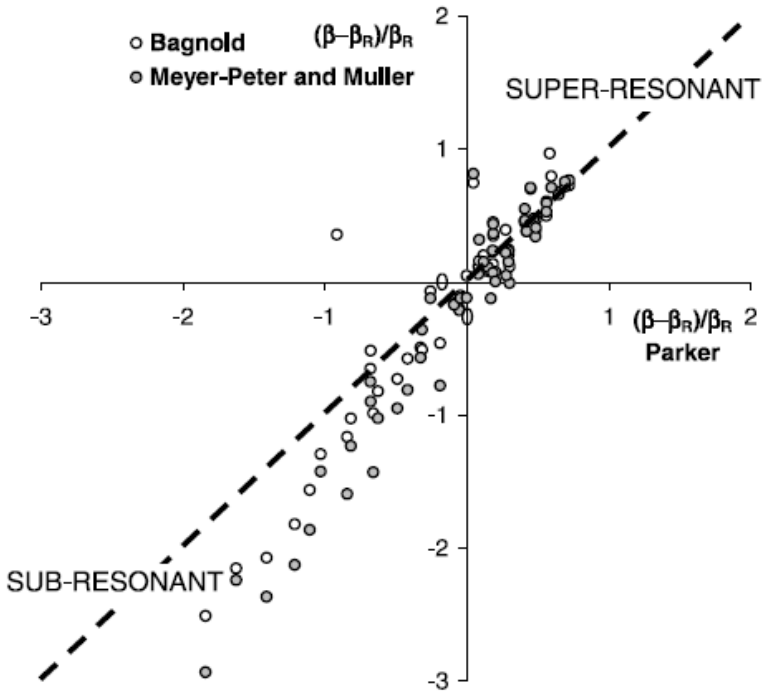


**Figure 4. Sensitivity of the morphodynamic regime indicator $(\beta_R - \beta)/\beta_R$ to the choice of different bed load predictors. The value of $(\beta_R - \beta)/\beta_R$ obtained using the *Parker* [1990] formula is reported on the horizontal axis, while the corresponding values obtained through the *Bagnold* [1980] and *Meyer-Peter and Miiller* [1948] formulae are reported along the vertical axis and denoted with white and grey circles, respectively.**

Table 3. Summary of the Results of the Analysis of Possible Morphodynamic Transitions

| | To Subresonant | To Superresonant |
|---|---|---|
| From subresonant | 30 (35%) | 0 (0%) |
| From superresonant | 42 (49%) | 14 (16%) |

in channel sinuosity that is suddenly reversed through bend cutoffs. For alluvial meanders this process takes place at a much faster timescale than any geomorphic process by which the longitudinal valley slope is adjusted. This implies a continuous variation of the down-channel slope at the timescale of the planimetric evolution of the meander bends, which causes a variation in the reach-averaged characteristics that define the regime of morphodynamic influence. This is accounted for in simulation models of river meanders through relations (7). Notice also that channel width may be expected to adjust to the gradually changing channel slope [e.g., *Millar,* 2005], provided meander evolution occurs at timescales slow enough with respect to that required to achieve the dynamic equilibrium [e.g., *Leopold and Maddock,* 1953; *Eaton et al.,* 2004]. Such an effect is not presently incorporated in the meander simulation model (nor in most others) and it is not likely to qualitatively affect the results presented below. Indeed, equation (13a) of *Millar* [2005] suggests that accounting for width adjustment to slope changes would imply a relatively faster temporal decrease of the width to depth ratio which would reinforce the qualitative outcomes presented below.

[51] In the present paragraph we seek to quantify to what extent the tendency of a single-thread channel to develop mature meanders can cause temporary time shifts in its morphodynamic regime. In order to do that we perform a series of planimetric evolution simulations from nearly straight initial planforms until cutoff, by solving the system (5)-(6). Input quantities are the reference dimensionless parameters of the reduced data set, as described at the end of section 3.2. In order to achieve a closer correspondence with field data, since the given data refer to river reaches with sinuosities exceeding unity, measured reach-averaged values of $\beta$, $\tau*$,$d_s$) have been properly rescaled to unit sinuosity through equations (7), which have been used to determine the initial values $\beta$ (0), $\tau*$ (0), $d_s$ (0) used in the simulations.

[52] The results are summarized in Table 3. Almost half (49%) of the examined river reaches tend to keep within the initial morphodynamic regime, while transitional streams almost invariably move from superresonant to subresonant conditions. The relatively high number of observed super-resonant to subresonant transitions is conditioned by the

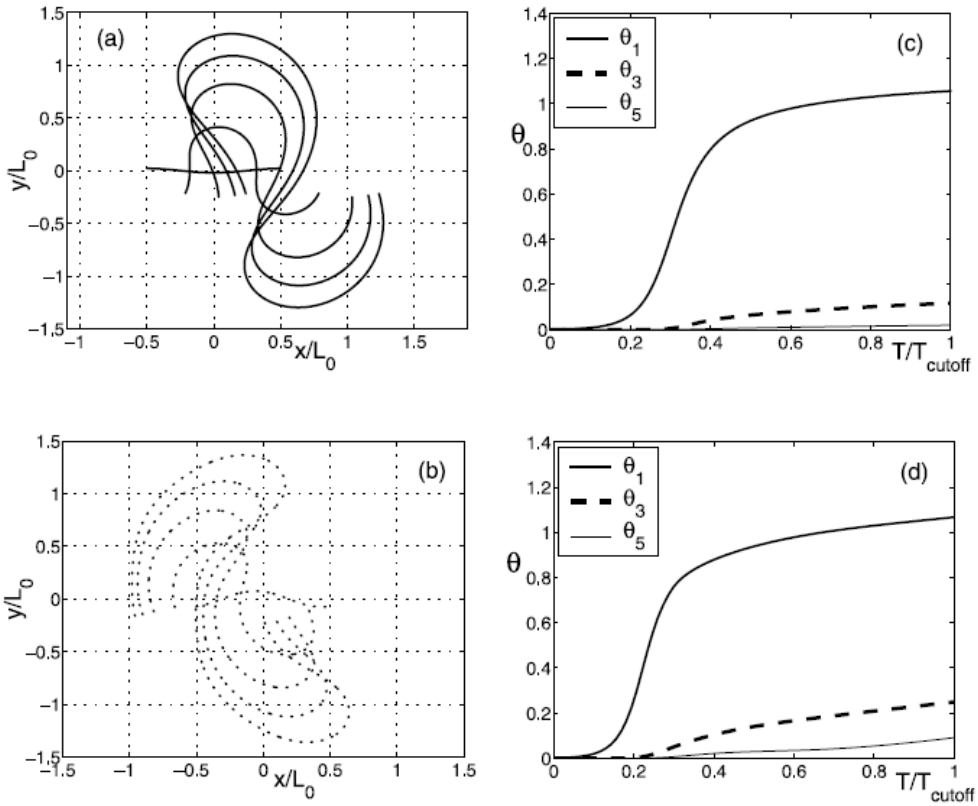


**Figure 5. Evolution (left) of meander planform and (right) of the amplitude (modulus) of $\vartheta_1, \vartheta_3, \delta_5$ when the regime keeps (a, c) subresonant and (b, d) superresonant. Figures 5a and 5c show that subresonant and superresonant planform evolution are characterized by opposite skewing of meander bends. The right plots also indicate that in both cases the assumption $|\vartheta_1| \gg |\vartheta_3| \gg |\vartheta_5|$ is verified.**

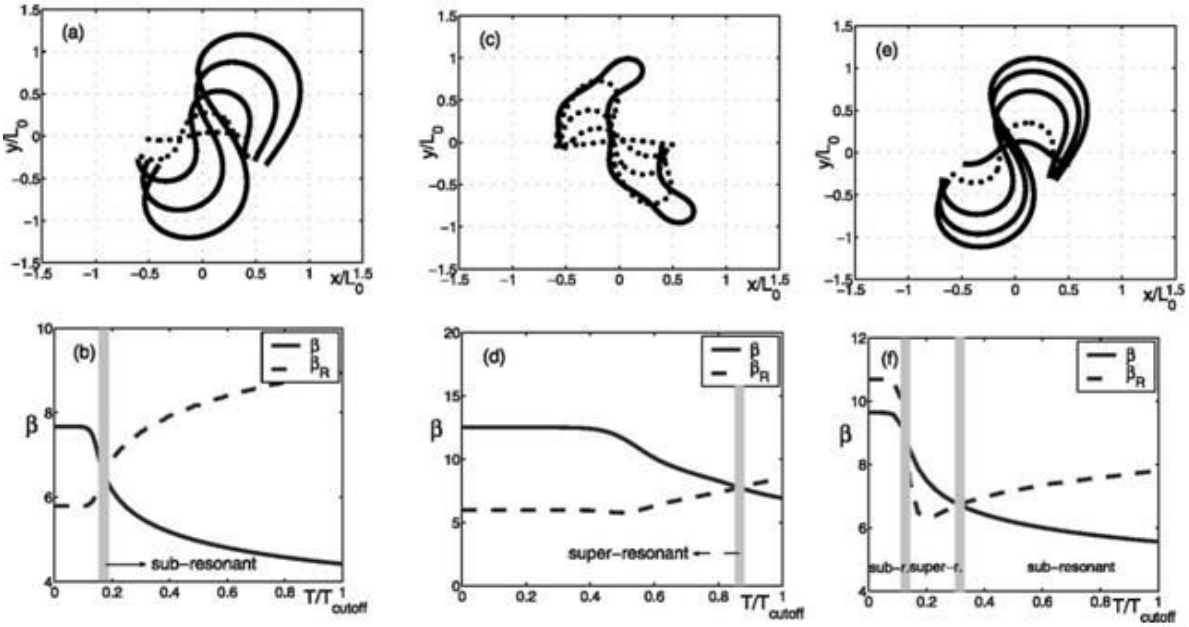


**Figure 6. Superresonant to subresonant transition (a, b) at low sinuosity, (c, d) at high sinuosity, and (e, f) subresonant evolution with limited superresonant window. Figures 6a, 6c, and 6e represent subsequent planforms, with solid and dotted lines denoting subresonant and superresonant conditions, respectively. Figures 6b, 6d, and 6f represent the time evolution of $\beta$ and of $\beta_R$.**

prevalence of initially superresonant reaches in the input data set (56 out of 86 reaches); absolute numbers of the observed transitions should be taken with some care since this result might be affected by the tendency of the simulation model to overestimate channel sinuosity *[Lanzoni et al.,* 2006].

[53] Figures 5a and 5b shows typical meandering plan-forms for reaches maintaining their initial morphodynamic regime. They are upstream skewed and migrate downstream in the subresonant regime (Figure 5a); the opposite behavior applies when $\beta > \beta_R$(Figure 5b). Note also that in this and following figures all the superresonant planforms are represented by a dotted line in order to illustrate more intuitively when morphodynamic transitions occur. The amplitude of the odd harmonics respects the assumption that $|\vartheta_5| \ll |\vartheta_3| \ll |\vartheta_1|$ at any evolution time; the presence of $\vartheta_3$ accounts for the skewing of meander shape and the absence of multilobing is reflected by the very small values attained by $\vartheta_5$ (Figures 5c and 5d).

[54] Different scenarios occur when the time evolution of $\beta$ and $\beta_R$ is such that the condition $\beta = \beta_R$ is attained at least once before the occurrence of cutoff. Sixty-five percent of the 86 examined rivers began to evolve with $\beta > \beta_R$ and for 75% of the initially superresonant stream reaches the scenario was reversed at cutoff. Transitions can occur when the channel sinuosity is low or high, but not when it has an intermediate value. Related examples of planform evolution are reported in Figures 6a, 6c, and 6e. Note that the superresonant planforms of Figure 6a show upstream migration, a tendency which is reversed at relatively low values of channel sinuosity ($T/T_{cutoff} \simeq 0.18'$, Figure 6b). In contrast, the typical upstream migration and downstream skewed meander shape of the superresonant regime is observed for most of the evolution time in Figure 6c, until $T/T_{cutoff} \simeq' 0.87$ (Figure 6d). Indeed, in both cases, after an initial constant region, the width ratio monotonically decreases as predicted by equation (7) while the resonant threshold almost invariably increases. Its temporal growth is basically related to the structure of the bed load relationship at relatively low Shields stress: the coefficient $\Phi_T$ is constant within this range, but increases monotonically with $\tau^*$for higher values of the Shields stress. Despite qualitative similar trends in $\beta(T)$ and $\beta_R(T)$, river planforms in Figures 6a and 6c are markedly different because they experience transition from the superresonant to the subresonant regime at much different evolution stages relative to cutoff.

[55] Nearly one fifth of the initially subresonant rivers exhibit a peculiar evolution dynamics, which keeps subresonant for almost all the evolution time. For this reason in Table 3 they are included in those rivers that keep within the subresonant regime. These streams experience a relatively narrow superresonant window for $T/T_{cutoff}$ in the approximate range 0.15-0.3 in Figure 6f. The corresponding, superresonant river planform is represented by the dotted line in Figure 6e. Figure 6f indicates that this is related to the initial decrease of $\beta_R$ followed by its growth due to the condition $\Phi_T$= *const* at low $\tau*$.

[56] The multilobed meander shapes of Figure 6c are related to the role of the fifth harmonic $\vartheta_5$, which commonly remains negligible before cutoff (Figures 5c, 5d, and 7a). The elongated, nearly multilobed pattern of Figure 6c is associated with a relatively rapid growth of $\vartheta_5$ that may be triggered (Figure 7b) when $\beta$ approaches $\beta_R$ (Figure 6d).

[57] But which conditions can be responsible for triggering the growth of $\vartheta_5$? In the absence of geometric non-linearities, the explanation would be rather simple. In this hypothetical case, the growth of each harmonic($\vartheta_1$, $\vartheta_3$,, $\vartheta_5$,) would be purely exponential in time *[Seminara et al.,* 2001, equation (3.6)]. This growth would be also greatly accelerated for $\lambda_j$ ($j = 1,3,5$)approaching the resonant wave number $\lambda_R$ corresponding to reach averaged conditions whereby $\beta = \beta_R$. At the beginning of each simulation $\lambda_1$equals the linearly most unstable intrinsic meander wavelength for the given values of $\big(\beta(0), \tau*(0), d_s(0)\big)$; at this stage the third and fifth harmonic are linearly stable, since they correspond to longer, nonamplifying meander wavelengths (see Figure 1). As a meander elongates the third and fifth harmonics progressively move toward the linearly unstable wavelength range. The relatively fast growth of $\vartheta_5$ starts around $T/T_{cutoff} \simeq 0.8$, when $\beta$ approaches $\beta_R$ (Figure 7b); at this stage, $\lambda_5 < \lambda_R$ but it is still close enough to resonance and therefore with a relatively high linear growth rate, which accelerates the growth of $\vartheta_5$ until later inhibited by geometric nonlinearities.

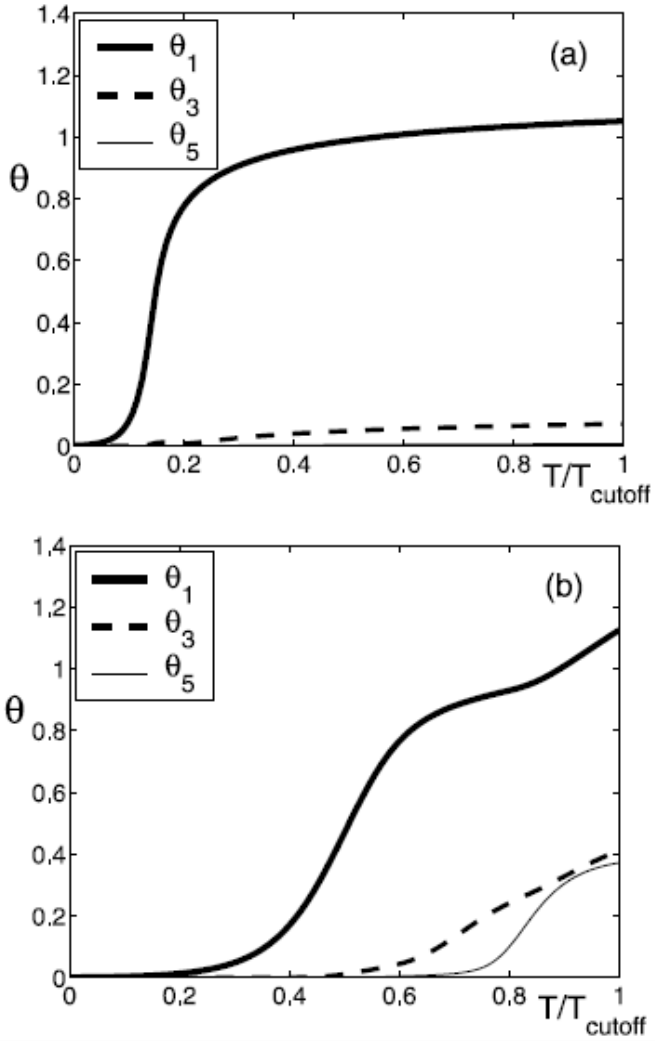


**Figure 7. Evolution of $|\vartheta_1|, |\vartheta_3|, |\vartheta_5|$ for superresonant to subresonant transitions at (a) low and (b) high sinuosities. Figure 7a refers to the meander evolution of Figure 6a: the planform skewing is related to the third harmonic $\vartheta_3$. Figure 7b refers to the meander evolution of Figure 6c: the tendency to multilobing is due to the fifth harmonic $\vartheta_5$ which, unlike in most cases, attains values comparable to $\vartheta_3$close to cutoff occurrence.**

[58] Figure 8 shows the possible morphodynamic transitions in relationship with the given values of the aspect ratio and of the Shields stress within the gravel bed rivers data set. The aspect ratio seems the main controlling parameter, while no relevant association can be made between the value of the Shields stress and the observed behaviors. Morphodynamic transitions can be expected for the range $8< \beta < 12$, which is the range just larger than the resonant range of Figure 3. Morphodynamic transitions are almost invariably (but not always) associated with a temporal growth of the resonant width to depth ratio, as indicated by the grey triangles; a prevailing temporal increase of $\beta_R$ is instead the condition that most effectively keeps a stream reach in its original subresonant regime, although opposite cases can be observed. Almost no correlation can be established, in contrast, between the time development of $\beta_R$ and the tendency of a superresonant stream reach to remain in its own state.

## 6. Discussion and Conclusions

[59] An assessment of the morphodynamic influence regimes (subresonant and superresonant [see *Zolezzi and Seminara,* 2001]) has been extensively examined in the case of gravel bed rivers for the first time. A well known

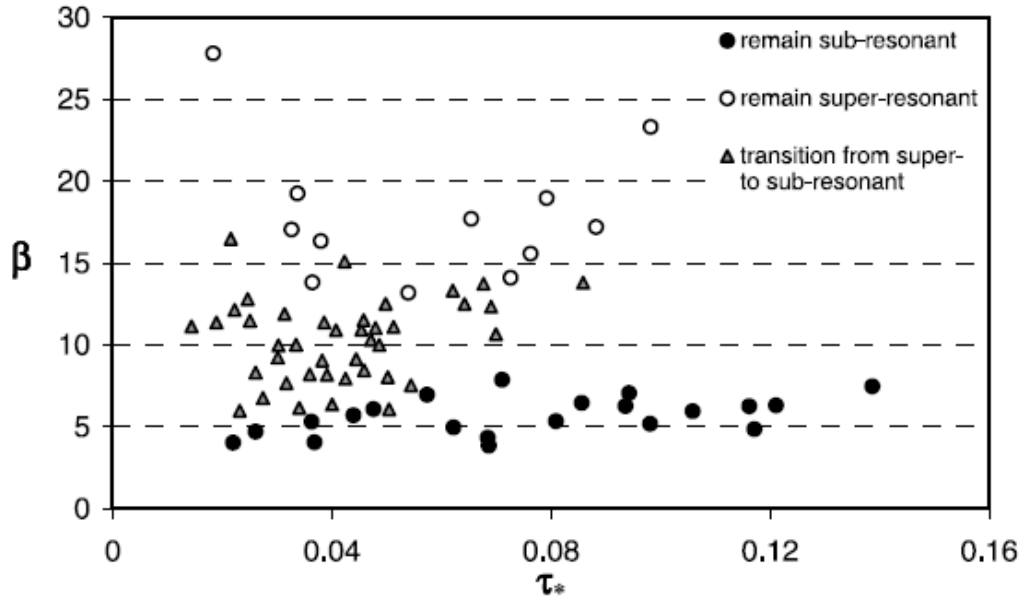


**Figure 8. Possible morphodynamic transitions in the $\beta - \tau^*$ plane.**

morphodynamic model has been applied to a data set recently used also by *Parker et al.* [2007] to support evidence of quasi-universal bankfull geometry relationships for gravel bed streams.

**[60]** Both regimes have been found to characterize single thread gravel bed rivers, with many more streams in the examined data set being superresonant. Application of *Parker et al.*'s [2007] bankfull hydraulic geometry relations to the computation of resonance conditions confirms the observed quasi-universal tendency of gravel bed rivers at low $\tau^*$ to behave superresonantly. The threshold width ratio (half width to depth ratio $\beta$) range separating the two behaviors is relatively narrow considering the degree of scatter in the input parameters. On this basis it can be suggested that reaches with $\beta < 7.5$ are probably subresonant while relatively wider and shallower gravel bed streams should behave superresonantly. Of course this should be taken as a rule of thumb that needs to be verified more rigorously through the computation of resonance conditions based on measured reach-averaged characteristics.

[61] The present work also provides some insight into which environmental factors can be responsible for the morphodynamic regime of a river reach. A possible perspective is to focus on the role played by autogenic and allogenic factors. The superresonant behavior has been observed to characterize streams with relatively high sediment supply, poorly vegetated and low-cohesion channel banks, which typically correspond to relatively shallow and wide channels. Moreover, higher sediment size and lower values of the Shields stress tend to reduce the resonant value $\beta_R$. To the extent that the above features can be considered inherent characteristics of gravel bed channels, the above observations would imply an inherent, or autogenic tendency of gravel bed streams to behave superresonantly.

[62] Variations in the characteristics of climate, the reach location along the river longitudinal profile, the sediment supply as well as anthropic effects able to modify bank strength might determine a subresonant shift within the above picture. According to well established knowledge, channel width ratio b might be reduced within more humid climates associated with denser bank vegetation as well as by a reduced sediment supply. Moving toward the lower part of the longitudinal river profile tends to promote larger values of the bankfull Shields stress $\tau *$and lower values of the relative roughness$d_s$, with a consequent increase in $\beta_R$.

[63] Moreover, it is pointed out that the possible dynamic nature of the morphodynamic regime in the case of developing meanders. Down-channel slope reduction due to meander elongation represents a further autogenic factor able to change the morphodynamic regime of a river reach due to evolving sinuosity. Almost invariably it is observed that transitions from the superresonant to the subreso-nant regime. In this respect anthropic factors such as levee and bank protection works as well as other sinuosity inhibitors like the frequent occurrence of chute cutoffs can be responsible for

deviation from the patterns observed of morphodynamic transitions referring to simple, sine-generated meandering planforms.

[64] The present results have been obtained on the basis of a relatively large number (134) of single-thread river reaches, which can be assumed to be representative of the hydraulic and geometric conditions typical of gravel bed rivers *[Parker et al.,* 2007]; nevertheless, the suggested scenarios should be tested with data from other geographical and geological settings, in order to check the possible effect of regional trends and constraints.

[65] It is pointed out that a complete validation of the present results would require the field observation of upstream and downstream morphodynamic influence and their direct correlation to the river reach being in superresonant and subresonant regimes, respectively. Field evidence of this behavior has never been documented so far and therefore represents a challenging issue for future research. Finally, a similar work referred to single-thread sand bed rivers would be of great interest to extend the present picture to river reaches whose morphodynamics is controlled by sediment transport dominantly occurring as suspended load, an issue that has received relatively little attention so far *[Federici and Seminara,* 2003].

**References**


Bagnold, R. (1980), An empirical correlation of bedload transport rates in flumes and natural rivers, *Proc. R. Soc. London, 372,* 453-473.

Blondeaux, P., and G. Seminara (1985), A unified bar-bend theory ofriver meanders, *J. Fluid Mech., 112*, 363-377.

Briggs, R. (1964), *Electron-Stream Interaction With Plasmas,* MIT Press, Cambridge, Mass.

Camporeale, C., P. Perona, A. Porporato, and L. Ridolfi (2007), Hierarchy of models for meandering rivers and related morphodynamic processes, *Rev. Geophys, 45,* RG1001,

Charlton, F. G., P. M. Brown, and R. W. Benson (1978), The hydraulic geometry of some gravel rivers in britain, *Rep. INT 180,* Hydraul. Res.Stn., 48 pp., Wallingford, U.K.

Chen, D., and J. Duan (2006), Modeling width adjustment in meandering channels, *J. Hydrol., 321,* 59-76.

Colombini, M., G. Seminara, and M. Tubino (1987), Finite-amplitude alternate bars, *J. Fluid Mech., 181,* 213-232.

Colombini, M., M. Tubino, and P. Whiting (1992), Topographic expression of bars in meandering channels, in *Dynamics of Gravel Bed Rivers,* pp. 457-474, edited by P. Billi et al., John Wiley, Chichester, N. Y.

Crosato, A. (1989), Meander migration prediction, *Excerpta, 4,* 169-198.

Crosato, A. (1990), Simulation of meandering river processes, *Commun. Hydraul. Geotech. Eng. 90-3,* 104 pp., Delft Univ. of Technol., Delft, Netherlands.

Darby, S. E., A. M. Alabyan, and M. J. Van de Wiel (2002), Numerical simulation of bank erosion and channel migration in meandering rivers, *Water Resour. Res.,* 38(9), 1163,

De Vries, M. (1965), Considerations about non-steady bed-load transport in open channels, *Proceedings IAHR Congress,* Paper 3.8, Int. Assoc. of Hydraul. Res., St. Petersburg, Russia.

Eaton, B., M. Church, and R. Millar (2004), Rational regime model of alluvial channel morphology and response, *Earth Surf. Processes Land-forms,* 29(4), 511-529.

Federici, B., and G. Seminara (2003), On the convective nature of bar instability, *J. Fluid Mech., 487,* 125-145.

Ferguson, R. I. (1984), Kinematic model of meander migration, in *River Meandering, Proceedings of Rivers '83,* edited by C. M. Elliott, pp. 942 -951, Am. Soc. of Civ. Eng., Reston, Va.

Frothingham, K., and B. Rhoads (2003), Three-dimensional flow structure and channel change in an asymmetrical compound meander loop. Em-barras River, Illinois., *Earth SurfProcesses Landforms, 28,* 625 -644.

Garcia, M., and Y. Nino (1993), Dynamics of sediment bars in straight and meandering channels: experiments on the resonance phenomenon,*J. Hydraul. Res., 31,* 739-761.

Gautier, E., D. Brunstein, P. Vauchel, M. Roulet, O. Fuertes, J. Darrozes, and L. Bourrel (2007), Temporal relations between meander deformation, water discharge and sediment fluxes, floodplain of the Rio Beni (Bolivian Amazonia)., *Earth Surf. Processes Landforms, 32*(2), 230 -248,doi:10.1002/esp1394.

Gay, G., H. Gay, W. Gay, H. Martinson, R. Meade, and J. Moody (1998),Evolution of cutoffs across meander necks in Powder River, Montana, USA, *Earth Surf. Processes Landforms, 23,* 651 –662.

Hasegawa, K. (1989), Studies on qualitative and quantitative prediction of meander channel shift, in *River Meandering, Water Res. Monogr.,* vol. 12, edited by S. Ikeda and G. Parker, pp. 215-235, AGU, Washington, D. C.

Hey, R. D., and C. R. Thorne (1986), Stable channels with mobile gravelbeds, *J. Hydraul. Eng., 112*(6), 671 – 689.

Hooke, A. (1995), Processes of channel planform changes on meandering channels in the UK, in *Changing*

*River Channels,* edited by A. Gurnell and G. Petts, pp. 87-116, John Wiley, Chicester, U.K.
Hooke, J. (2003), River meander behaviour and instability: A framework for analysis., *Trans. Inst. Br. Geogr., 28,* 238 -253.
Hooke, J. (2007a), Spatial variability, mechanisms and propagation of change in an active meandering river, *Geomorphology, 84,* 277 -296.
Hooke, J. (2007b), Complexity, self-organization and variation in behaviour in meandering rivers, *Geomorphology, 91,* 236-258, doi:10.1016/j.geomorph.2007.04.021.
Hooke, J., and C. Redmond (1989), River-channel changes in England and Wales, *J. Inst. Water Environ. Manage., 3,* 328 -335.
Howard, A. (1996), Modelling channel evolution and floodplain morphology, in *Floodplain Processes,* edited by P. A. Carling and G. E. Petts, pp.15 -62, John Wiley, Chicester, U.K.
Ikeda, S., G. Parker, and K. Sawai (1981), Bend theory of river meanders. Part 1 - Linear development, *J. Fluid Mech., 112,* 363-377.
Johannesson, H., and G. Parker (1989), Linear theory of river meanders, in n*River Meandering, Water Res. Monogr.,* vol. 12, edited by S. Ikeda and
G. Parker, pp. 181-214, AGU, Washington, D. C. Kellerhals, R., C. Neill, and D. Bray (1972), Hydraulic and geomorphic characteristics of rivers in Alberta, technical report, Alberta Coop. Res. Program in Highway and River Eng., Edmonton, Canada.
Kinoshita, R. (1961), An investigation of channel deformation of the Ishi-kari River, technical report, Nat. Resour. Div., Minist. of Sci. and Tech- nol. of Jpn., Tokyo.
Kondolf, G. (2006), River restoration and meanders, *Ecol. Soc., 11*(2), 42.
Kuroki, M., and T. Kishi (1985), Regime criteria on bars and braids, *Tech. Rep. 14,* Hokkaido Univ., Sapporo, Japan.
Langbein, W. B., and L. B. Leopold (1964), Quasi equilibrium states in channel morphology, *Am. J. of Sci., 262,* 782 - 794.
Lanzoni, S., and G. Seminara (2006), On the nature of meander instability, *J. Geophys. Res., 111,* F04006, doi:10.1029/2005JF000416.
Lanzoni, S., A. Siviglia, A. Frascati, and G. Seminara (2006), Long waves in erodible channels and morphodynamic influence, *Water Resour. Res.,* 42, W06D17, doi:10.1029/2006WR004916.
Leopold, L., and J. Maddock (1953), The hydraulic geometry of stream channels and some physiographic implications, *U. S. Geol. Surv. Prof. Pap., 252,* 57 pp.
Lyn, D., and M. Altinakar (2002), St.Venant Exner equations for near-critical and transcritical flows, *J. Hydraul. Eng., 128*(6), 579-587.
Meyer-Peter, E., and R. Miiller (1948), Formulas for bed-load transport, paper presented at 2nd Congress International Association for Hydraulic Research, Stockholm, Sweden.
Millar, R. (2000), Influences of bank vegetation on alluvial channel patterns, *Water Resour. Res.,* 36(4), 1109-1118.
Millar, R. (2005), Theoretical regime equations for mobile gravel-bed rivers with stable banks, *Geomorphology, 67,* 204-220, doi:10.1016/j.geomorph.2004.07.001.
Mosselman, E., G. Zolezzi, and M. Tubino (2006), The overdeepening theory in river morphodynamics: Two decades of shifting interpretations, in *River Flow 2006 Proceedings of the International Conference on Fluvial Hydraulics, Lisbon, Portugal, 6-8 September 2006,* edited by R. M. L. Ferreira et al., pp. 1175-1181, Taylor and Francis, London.
Nagata, N., T. Hosoda, Y. Muramoto, and M. Rahman (1997), Experimental and numerical studies in meandering channels with bank erosion, in paper presented at the Conference on Management of Landscape Disturbed by Channel Incision, Univ. of Miss., University.
Nobile, G., M. Bolla Pittaluga, and G. Seminara (2008), A non-linear model for river meandering, paper presented at RCEM 2007, 5th IAHR Symposium on River, Coastal and Estuarine Morphodynamics, Univ. of Twente, Enschede, Netherlands, 17 -21 Sept.
Parker, G. (1979), Hydraulic geometry of active gravel rivers, *J. Hydraul. Div. Am. Soc. Civ. Eng.), 105,* 1185-1201.
Parker, G. (1990), Surface-based bedload transport relation for gravel rivers, *J. Hydraul. Res., 28,* 417-436.
Parker, G., P. Displas, and J. Akiyama (1983), Meanders bends of high amplitude, *J. Hydraul. Eng., 109,* 1323 -1337.
Parker, G., C. Toro-Escobar, M. Ramey, and S. Beck (2003), The effect of flood water extraction on the morphology of mountain streams, *J. Hydraul Eng., 129,* 885-895.
Parker, G., P. R. Wilcock, C. Paola, W. E. Dietrich, and J. Pitlick (2007),Physical basis for quasi-universal relations describing bankfull hydraulic geometry of single-thread gravel bed rivers, *J. Geophys. Res., 112,* F04005, doi:10.1029/2006JF000549.
Perucca, E., C. Camporeale, and L. Ridolfi (2005), Nonlinear analysis of the geometry of meandering

rivers, *Geophys. Res. Lett., 32,* L03402, doi:10.1029/2004GL021966.
Pitlick, J., and R. Cress (2000), Longitudinal trend in channel characteristics of the colorado river and implications for food-web dynamics, technical report, U. S. Fish and Wildlife Serv., Grand Junction, Colo.
Ruther, N., and N. Olsen (2007), Modelling free-forming meander evolution in a laboratory channel using three-dimensional computational fluid dynamics, *Geomorphology, 89,* 308-319, doi:10.1016/j.geomorph. 2006.12.009.
Seminara,G. (2006),Meanders,*J. Fluid. Mech, 554*,271 -297,doi:10.1017/ S0022112006008925.
Seminara, G., and M. Tubino (1989), Alternate bars and meandering: Free, forced and mixed interactions, in *River Meandering, Water Res. Monogr.,* vol. 12,editedbyS. IkedaandG. Parker,pp. 267-320,AGU,Washington,D. C.
Seminara, G., and M. Tubino (1992), Weakly nonlinear theory of regular meanders, *J. Fluid Mech., 244,* 257-288.
Seminara, G., G. Zolezzi, M. Tubino, and D. Zardi (2001), Downstream and upstream influence in river meandering. Part 2. Planimetric development, *J. Fluid Mech., 438,* 213-230.
Struiksma, N., K. Olesen, C. Flokstra, and H. de Vriend (1985), Bed deformation in curved alluvial channels, *J. Hydraul. Res., 23*(1), 57-79.
Sun, T., P. Meaking, and T. Jossang (2001), A computer model for meandering rivers with multiple bed load sediment sizes: 1. Theory, *Water Resour. Res., 37*(8), 2227-2241.
Van den Berg, J. (1995), Prediction of alluvial channel pattern of perennial rivers, *Geomorphology, 12,* 259-279.
Zolezzi, G., and G. Seminara (2001), Downstream and upstream influencein river meandering. Part 1. general theory and application of overdee-pening, *J. Fluid Mech., 438,* 183-211.
Zolezzi, G., M. Guala, D. Termini, and G. Seminara (2005), Experimental observation of upstream overdeepening, *J. Fluid Mech., 531,* 191 -219.